SCIENTIFIC REPORTS

OPEN

SUBJECT AREAS:
NANOPARTICLES
ORGANIC-INORGANIC NANOSTRUCTURES
ENVIRONMENTAL MONITORING
SENSORS AND BIOSENSORS

Received
21 March 2013

Accepted
6 June 2013

Published
27 June 2013

Correspondence and requests for materials should be addressed to K.K.N. (nanda@mrc.iisc.ernet.in)

Nanocomposite based flexible ultrasensitive resistive gas sensor for chemical reactions studies

Sadanand Pandey, Gopal K. Goswami & Karuna K. Nanda

Materials Research Centre, Indian Institute of Science, Bangalore 560012, India.

Room temperature operation, low detection limit and fast response time are highly desirable for a wide range of gas sensing applications. However, the available gas sensors suffer mainly from high temperature operation or external stimulation for response/recovery. Here, we report an ultrasensitive-flexible-silver-nanoparticle based nanocomposite resistive sensor for ammonia detection and established the sensing mechanism. We show that the nanocomposite can detect ammonia as low as 500 parts-per-trillion at room temperature in a minute time. Furthermore, the evolution of ammonia from different chemical reactions has been demonstrated using the nanocomposite sensor as an example. Our results demonstrate the proof-of-concept for the new detector to be used in several applications including homeland security, environmental pollution and leak detection in research laboratories and many others.

Ammonium nitrate is present in many explosives and is known to gradually decompose and release trace amounts of ammonia. It is, therefore, essential to detect a trace of the gas to prevent the fatal accidents. The variation of conductivity of metal oxides and conducting polymers has been explored for the detection of ammonia in ppb (parts-per-billion) range. The conventional solid state and conducting polymer sensors suffer from ultralow detection at room temperature[1–26]. The commercially available conducting polymer sensors require high power consumption since they provide adequate sensitivity only at high temperatures. Intense research is underway to develop new sensing materials and devices for a wide range of applications, especially, at room temperature. It has been shown that the graphene and carbon nanotube based detectors can operate at room temperature[27–32]. However, it is required to supply air or oxygen along with ammonia and apply either a current of 100 mA or UV illumination in order to clean the adsorbed gas molecules for sensor recovery[27–32]. A self-activated highly sensitive graphene[32] or metal oxide nanostructures[33] have been reported where the response time is few minutes.

An ideal sensor should possess the following significant features: (i) operation at room temperature; (ii) working in ambient environment and no requirement of oxygen or air supply; (iii) no external stimulus such as Joule heating or UV illumination for response/recovery; (iv) low detection limit; (v) high sensitivity and reproducibility; (vi) fast response and recovery; (vii) low cost and eco-friendly, etc. We have previously reported the aqueous ammonia sensing of guar gum/silver nanoparticles (GG/Ag) solutions based on the variation of the surface plasmon resonance (SPR) peaks[34]. Limitations of the method are that the solution cannot be reused and the detection limit is ppm level. Here, we report an ultrasensitive chemiresistor sensor based on GG/Ag nanocomposite for ammonia detection. The conductance of the sensor increases and the change is shown to be improved by increasing the loading of Ag nanoparticles. Our experimental investigation reveals that GG and nanoparticle interface is an active site for ammonia sensing (GG alone cannot sense ammonia), and the environment especially oxygen play a significant role. Our experimental findings indicate that the sensor in all aspects qualifies to be considered as an excellent sensor. Sensitivity, stability, reproducibility and durability studies reveal excellent device properties that can be explored as ammonia sensor for explosive and medical applications. The most important advantages of the sensor are the room temperature operation in ambient and wide range of detection ranging from few parts-per-trillion (ppt) to few hundred ppm.

Results

Ammonia sensing study. The sensing properties of the GG/Ag nanocomposite films are tested against increasing ammonia concentration in the range of 500 ppt–1300 ppm by monitoring the changes in current through current (I)-voltage (V) measurements in ambient. Optical micrograph of the film I (obtained from 15 mM of

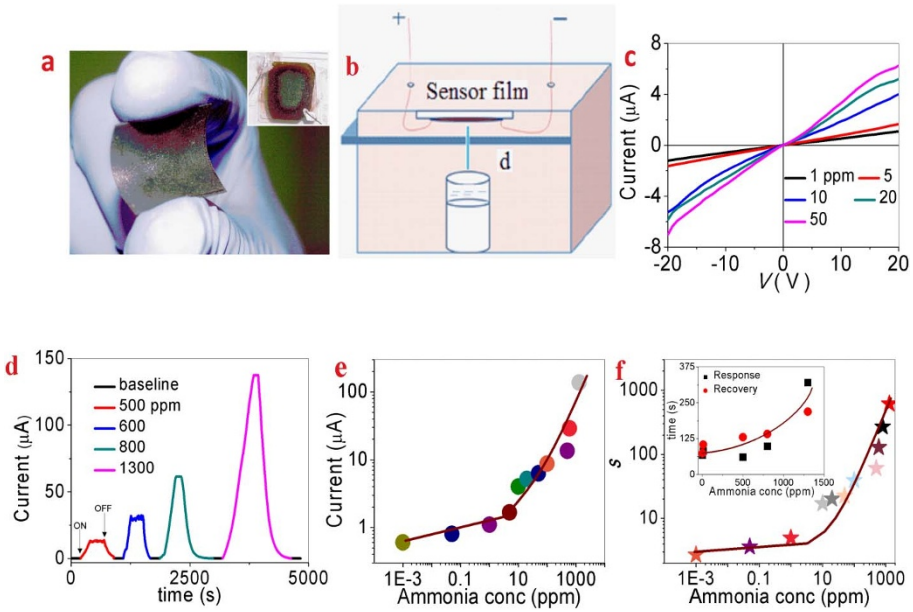

Figure 1 | Ammonia sensing of GG/Ag film I. (a) Optical micrograph of the film on a flexible substrate. Optical micrograph of the film with electrical leads is shown in the inset. (b) Schematic representation of the experimental set up. The distance from the source to film is 1 cm. (c) Current-voltage characteristics with different ammonia concentrations. (d) Temporal response to different ammonia concentrations for an applied voltage of 20 V. Ammonia ON and OFF are indicated by arrows. (e & f) Current and sensitivity as a function of ammonia concentration in log-log plot. Response time and recovery time are shown in the inset. Solid lines are guide to the eye.

Ag precursor) on a flexible substrate is shown in Fig. 1a. The sensor GG/Ag nanocomposite film with electrical leads is shown in the inset of Fig. 1a. The ammonia sensing experiments are carried out using a testing chamber as shown in Fig. 1b. It may be noted that ammonia gets generated from aqueous ammonia as $NH_4OH \rightarrow NH_3 + H_2O$. Figure 1c shows the *I-V* characteristics of film I at room temperature for different ammonia concentration. It is interesting to note that the current and hence, the conductivity increases when exposed to ammonia. In this context, it may be noted that the conductivity of porous silicon[35] and β-Fe_2O_3 nanoparticles[14] increases with the interaction of NH_3 molecules, while the conductivity decreases for chemiresistor films comprised of gold or platinum nanoparticles and 1,9-nonanedithiol[36] and Ag mesowires[18]. No change of current was observed for polysaccharide without Ag nanoparticles. Temporal response for different ammonia concentration is shown in Fig. 1d. The current is found to increase with the increase of ammonia concentration as shown in Fig. 1e.

It is evident that the sensing of ammonia vapor by the GG/Ag nanocomposite film has good reproducibility. Reproducibility with 800 ppm ammonia concentration for 3 cycles is shown in Supplementary Fig. S1. The sensitivity is defined as $s = \Delta\sigma/\sigma_0$, $\Delta\sigma = \sigma - \sigma_0$, where σ_0 and σ are the conductivity without and with ammonia exposure. Figure 1f shows the dependence of ammonia concentration on the sensitivity of film I. It can be noted that the sensitivity increases in the wide range of concentration. This is in good agreement with the theoretical prediction of sensitivity of resistive sensor that is proportional to the concentration of the analyte[35]. The response as well as recovery time are comparable and found to increase with the increase of ammonia concentration as shown in the inset of Fig. 1f[27].

Shown in Fig. 2a are the temporal responses of GG/Ag film II (obtained from 30 mM Ag precursor) to different ammonia concentration of 500 ppt, 50 ppb, 1 ppm, 20 ppm and 50 ppm. The current increases with ammonia concentration (Fig. 2b) as is the case with film I and the variation of sensitivity is shown in Fig. 2c. Interestingly, the sensitivity increased almost 1.5-fold with identical response and recovery time as for film I. The response of film II to 500 ppt clearly indicates that sub-ppb ammonia concentration can easily be detected. The response time is ~50 s. The response as well as recovery time are comparable and found to increase with the increase of ammonia concentration as is the case of film I and shown in Fig. 2d. It may be noted here that both the detection limit and the sensitivity can also be improved further by reducing the distance between the sensor and the source.

In order to test the durability and stability of the sensing properties, the films were aged at ambient conditions for several weeks and the response to 800 ppm was monitored. It is seen that the sensitivity decreases by 4% for 90 days aged film depicting the high stability of the films (Supplementary Fig. S2). It is also observed that the chemiresistor based ammonia sensing is found to be stable after several measurements. SEM images of the film taken after sensing studies (Supplementary Fig. S3) clearly reveals the stability of the film.

Discussion

It is well established for metal oxide semiconductors that oxygen chemisorbs on the sensor surface and the resistance changes are monitored with and without the analytes. In order to understand the mechanism associated with the GG/Ag nanocomposite film, the effect of different environment (ambient, nitrogen and oxygen) on the conductivity/current of film I has been studied. Temporal response in different ambient is shown in Fig. 3a,b. It can be noted from Fig. 3a that the current decreases in ambient for ~5 s and remains stable, while the current continues to decrease even after 100 s under the oxygen supply. However, the current does not change in nitrogen environment. The current decrease in ambient or oxygen may be due to the chemisorbed oxygen due to applied voltage. The decrease in the current in oxygen environment is almost four times more than in ambient. The extent of decrease in current possibly depends on the oxygen concentration. It may be noted that ambient environment contains ~21% oxygen which is four times lesser than 100% pure oxygen gas.

In another batch of experiments, ammonia sensing at 500 ppm were performed by sequential altering the environmental conditions

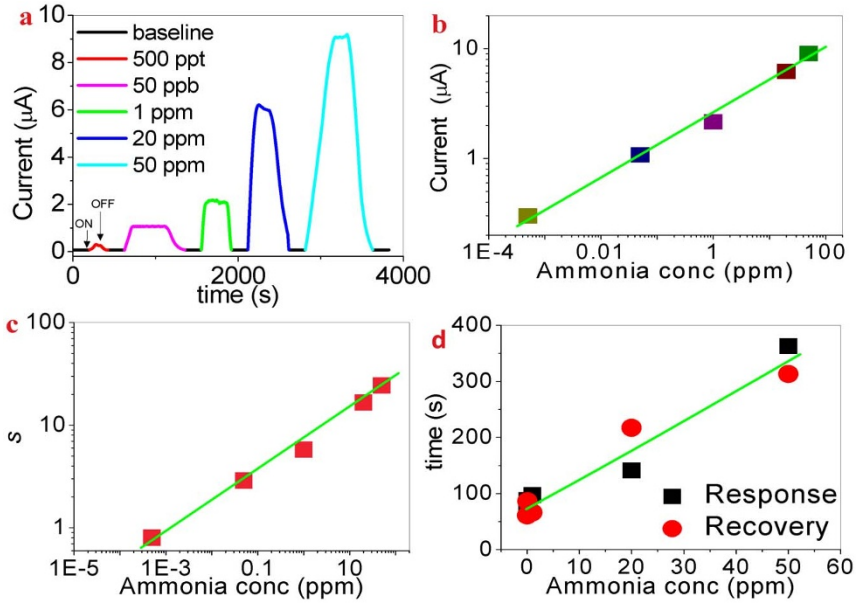

Figure 2 | Ammonia sensing of GG/Ag film II. (a) Temporal response to different ammonia concentrations. Ammonia ON and OFF are indicated by arrows. (b & c) Current and sensitivity as a function of ammonia concentration in log-log plot. Solid lines are guide to the eye. (d) Response time and recovery time as a function of ammonia concentration. Solid lines are guide to the eye.

and the results are presented in Fig. 3b. It is evident that the excellent repeatability in the sensor response and recovery both in ambient and in oxygen is observed with a greater than 99% recovery after 1–3 min. However, the sensor does not respond in nitrogen atmosphere even though the films are treated with oxygen plasma (Supplementary fig. S4). As the sensing behaviors are identical in ambient and oxygen environments, our sensor can be excellent ammonia detection in ambient environment.

Based on the experimental results, the plausible mechanism of ammonia sensing has been established. Chemisorptions of oxygen onto GG/Ag nanocomposite interface acts as an active species (Fig. 4) as is the case of metal oxide semiconductors. It is also seen that the sensitivity increases with the increase of Ag loading in the film. This signifies the more interfacial active sites available for oxygen adsorption and subsequent ammonia sensing. Here, the role of Ag nanoparticles could be the breaking of hydrogen bonding[37–39] and –OH groups so that the oxygen gets adsorbed onto interface of the GG/Ag nanocomposite as O_2^- (Fig. 4). The –OH groups free form hydrogen

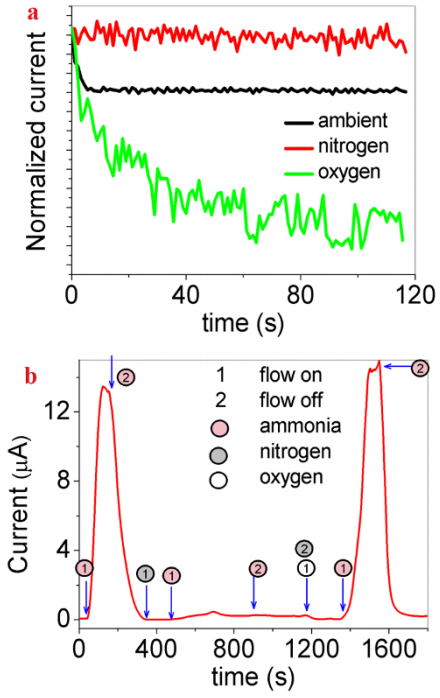

Figure 3 | Ammonia sensing at different environment. (a) Current stability and (b) ammonia sensing study at different environments; ambient, nitrogen and oxygen.

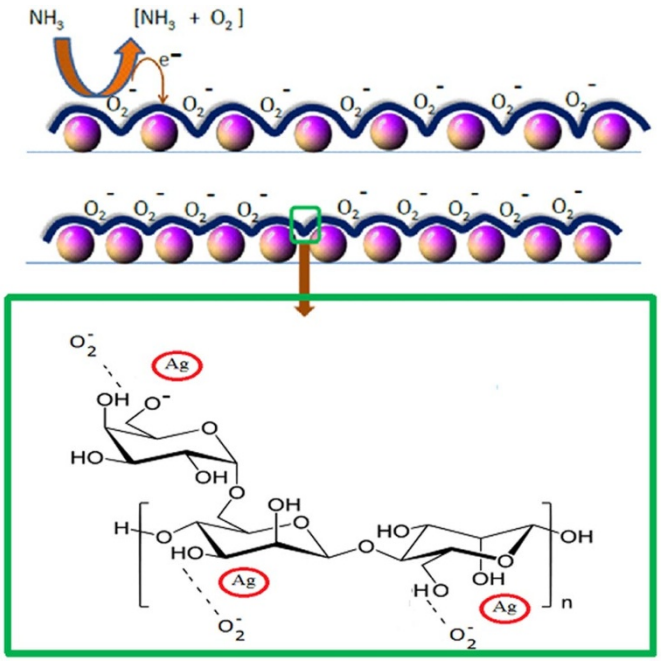

Figure 4 | Sensing mechanism. Oxygen chemisorbs on the sensor surface. The interfacial active sites are available for oxygen adsorption. Higher is the Ag loading, more is the active site for the oxygen adsorption, thereby increasing the sensitivity. When the sensor is exposed to ammonia, the oxygen gets released and the conductance/current increases.

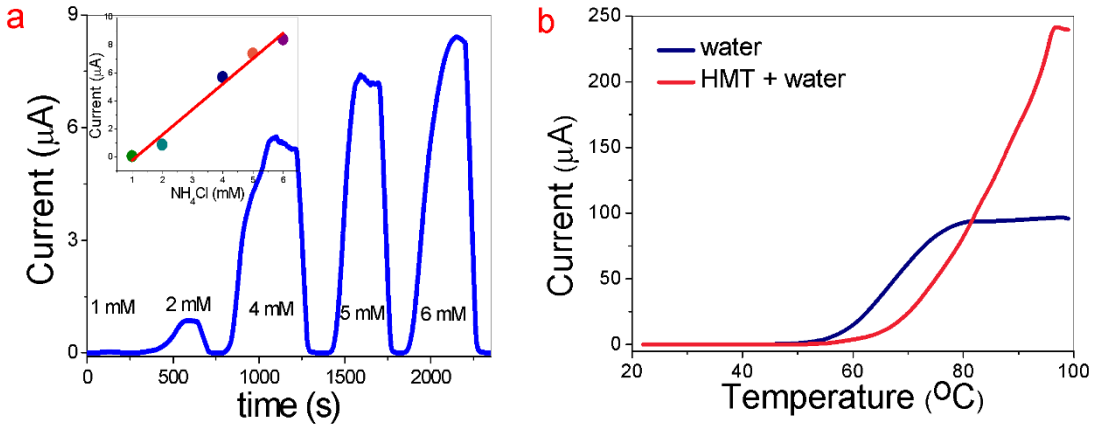

Figure 5 | Ammonia evolution from chemical reaction. (a) Temporal response of ammonia evolution for different NH_4Cl concentrations (1, 2, 4, 5, 6 mM). Current as a function of NH_4Cl concentration is shown in the inset. (b) Ammonia evolution from HMT as a function of temperature. The current is measured at a constant bias of 20 V.

bonding in the GG/Ag nanocomposite possibly get hydrogen bonded with O_2^-. The chemisorbed oxygen extracts electron from the sensor resulting in the decrease in current. It may be noted that the sensor behaves like *n*-type semiconductor (Supplementary Fig. S5) with an electron carrier concentration and mobility of $\sim 4.5 \times 10^{11}$ cm^{-3} and 4.6×10^4 $cm^2/V.s$, respectively. The incoming ammonia vapors take away the adsorbed oxygen releasing the electron to the sensor. Therefore, the current/conductivity increases with the exposure to ammonia. It was also observed that there is no response in nitrogen environment (Fig. 3c). Furthermore, we have obtained nearly the same atomic percentage (~1.4 at%) of nitrogen in the GG/Ag films before and after ammonia sensing experiment (Supplementary fig. S6). The results clearly depict that there is no direct interaction (either chemisorptions or physisorption) of ammonia with the sensing film. The presence of nitrogen can be attributed to the protein impurities (~5 wt%) present[40] in the commercial guar gum.

The influence of humidity on the ammonia sensing for GG/Ag nanocomposite film has been studied under different natural humidity (%RH) conditions (Supplementary fig. S7). A monotonic increase in the sensitivity (within 12%) is observed for a concentration of 500 ppm when the humidity is between 25 and 70%RH. This is expected for *n*-type materials due to the "donor effect" of water molecules[41–43]. Overall, the humidity has to be known for accurate detection of the ammonia concentration or else the senor should be calibrated at a humidity of 50%RH so that the variation in the sensitivity will be within 6%.

We have also carried out the sensing studies under flat and bending conditions. The *I-V* characteristics of film in nitrogen and ambient with different bending angles (0 to 40°) are shown in (Supplementary fig. S8a,b). The current through the film decreases in ambient environment while no change is observed in presence of nitrogen. This can be due to the stretching of the flexible film upon bending which increases the active interfacial sites for oxygen adsorption leading to a decrease in the current. The temporal response (Supplementary figure S8c,d) with different bending angles (0–40°) indicates that the sensitivity increases (about 7.5% upon bending of 0–20°) initially followed by a decrease in the sensitivity (about 22.7% for a bending angle of 40°). This can be understood by the initial increase in the active sites upon bending which increases the sensitivity of the film. At higher bending angle, the average distance between film and the analytes increases leading to a lower sensitivity of the film. Similar increase in the sensitivity of the sensor with the bending angle is being reported by other groups[44,45].

A clear demonstration of advanced functional properties of GG/Ag film for real-life applications of ammonia sensing has been performed. A fundamental well known chemical reaction in chemistry is used for ammonia evolution. Ammonia evolves when NH_4Cl reacts with NaOH. The reaction in equation (i) as:

$$NH_4Cl + NaOH \rightarrow NH_3 + NaCl + H_2O \quad \text{(i)}$$

It may be noted that one mole of NH_4Cl generate one mole of NH_3. Hence, the amount of NH_3 should be proportional to the amount of NH_4Cl. We have examined the ammonia evolution by increasing the concentration of NH_4Cl in the range of 1–6 mM and monitoring the changes in current. Figure 5a shows the temporal response of film I for different concentration of NH_4Cl. It is interesting to note that the current i.e. the amount of ammonia evolution increases linearly with the concentration of NH_4Cl as shown in the inset.

In another experiment, we examine a reaction proposed in the literature. It is believed that hexamethylenetetramine (HMT, $C_6H_{12}N_4$) decomposes by water to form formaldehyde and ammonia vapour above 60°C, which dissociates further to form ammonium cations and hydroxyl anions as shown in equation (ii)[46,47]:

$$\begin{aligned} &C_6H_{12}N_4 + 6H_2O \rightarrow 6H_2CO + 4NH_3 \\ &NH_3 + H_2O \rightarrow NH_4OH \rightarrow NH_4^+ + OH^- \end{aligned} \quad \text{(ii)}$$

HMT has been widely used in the preparation of oxides such as Co_3O_4, CeO_2, ZnO, CuO, ZrO_2 and HfO_2 nanostructures[48–54]. In this context, it may be noted that the growth of these oxides takes place above ~60°C. Surprisingly, no change in the current has been observed till the temperature of the solution reaches 60°C as shown in Fig. 5b. Above this temperature, there is a gradual increase in the current till 95°C beyond which it intends to saturate. It signifies the reaction starts at above 60°C that corroborates with the reported literature[46,47]. In the absence of HMT, the current increases above 45°C and saturates around 80°C. It may be noted the saturation current is almost half in the absence of HMT. The increase of current above 45°C may be due to water vapour evolves during heating. Over all, the kinetics of any laboratory reaction with ammonia or any other reducing gas evolution and any other harmful gases can easily be monitored.

To confirm the selectivity of the sensor, we have performed sensing studies for various organic vapors such as methanol (CH_3OH), ethanol (C_2H_5OH), acetone (C_3H_6O), carbon tetrachloride (CCl_4) and trichloroethylene (C_2HCl_3) as shown in Fig. 6. The concentration of all the analytes is 500 ppm. No change in current was observed and hence, the sensitivities are closed to zero for ethanol, methanol and acetone. On the other hand, the sensitivities for carbon tetrachloride and trichloroethylene are found to be 0.16 and 0.10 respectively which are much lower compared to ammonia (~60).

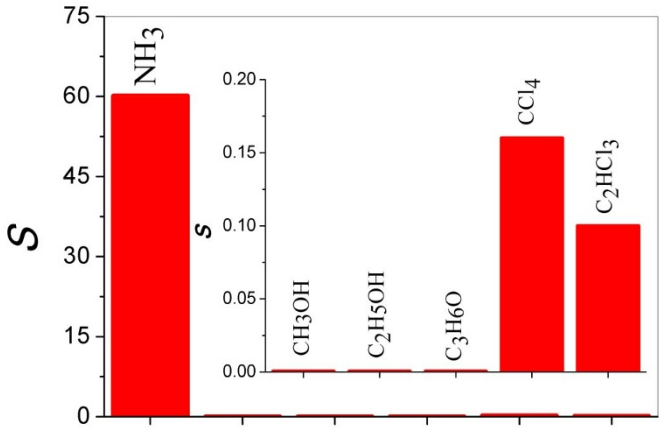

Figure 6 | Selectivity of the sensor. Selectivity of GG/Ag nanocomposite for ammonia sensing. Inset shows the response to different analytes. The concentration of different analytes is 500 ppm.

This suggests the selectivity of the sensor toward ammonia. Ammonia is known to be a strong reducing agent among the analytes investigated, takes away the chemisorbed oxygen present on the sensor surface efficiently resulting in a high sensitivity.

Ultimately, a sensor based on GG/Ag nanocomposite film has been developed which can not only be used for the detection of sub ppb but also for few hundred ppm. A sensing mechanism for the ammonia detection has been established which can also be applicable for other reducing analytes such as hydrogen, methane, etc. The main advantages of the sensor are its operation at room temperature over the wide range and working under ambient environment. Apart from this, the sensor does not require any external stimulus for response/recovery. The sensitivity, reversibility, stability and reproducibility of the sensors are superior as compared to the sensors reported in the literature. The conductance change is ~600 for a concentration of 1300 ppm. It has also been demonstrated that the sensor can be used for the investigation of ammonia evolution from chemical reactions. One of the most important advantages of the sensor is the change in current in μA range which can even be detected by a multimeter without using sophisticated source-measure-unit. The overall paramount performance of the sensor can conveniently be fixed into portable hand-held devices and could be deployed for a variety of applications, such as environmental monitoring, industrial applications such as in chemical processing plants, and homeland security for counter-terrorism, and leak detection in research laboratories.

Methods

Materials. $AgNO_3$ was purchased from Aldrich and used without farther purification. Guar gum was purchased from Merck, India. All aqueous solutions were made using ultrahigh purity water purified using a Mill-Q Plus system (Millipore Co.).

Preparation of GG/Ag nanocomposite. The precursors used to prepare Ag nanoparticles are GG and Ag nitrate. 2.5%w/v of GG was dissolved in 10 ml distilled water with the help of magnetic stirrer. After complete dissolution, the temperature of the reaction medium is raised to 70°C. Now 10 ml of 15 mM Ag nitrate solution was then added drop wise. The reaction mixture was kept under continuous stirring for 90 min. The synthesis takes place at pH 6. Short time after addition of Ag nitrate, the reaction medium acquires a clear yellow color indicating the formation of Ag nanoparticles. In order to make the double loading, 30 mM Ag nitrate are used, keeping all the conditions same. The details procedure has been reported elsewhere[34].

Characterization of GG/Ag nanocomposite. The GG/Ag nanocomposites were then characterized by X-ray diffraction (XRD) using Bruker D8 Advance powder diffractometer operating in the reflection mode with CuKα radiation. The morphology of the films was investigated by scanning electron microscope (SEM) using a FEI-SIRION. The size and shape of the nanoparticles were obtained using transmission electron microscope (TEM) with a TECHNAI T20 microscope. For TEM studies, the samples were prepared by directly dispersing the colloidal solution on a carbon coated copper grid. Fourier transform infrared spectroscopy (FTIR) spectrum was recorded in FTIR spectrophotometer (Spectrum-100, Perkin-Elmer, USA) to confirm the presence of the required functional groups in the GG and GG/Ag nanocomposite.

TEM image shown in Supplementary Fig. S3a reveals that Ag nanoparticles are spherical and encapsulated by the GG as shown in the inset of Supplementary Fig. S3a. The corresponding size distribution histogram obtained for 542 particles is shown in the inset of Supplementary Fig. S3a which clearly illustrates that the size of the particles is in the range of 4–14 nm with an average particle size of 8.5 nm. HRTEM images shown in Supplementary Fig. S3b & c indicate single crystalline particles with a lattice spacing of 0.237 nm, matching with the *d*-spacing in the (111) plane of Ag with a face-centered cubic (fcc) structure. SEM images of GG/Ag nanocomposite films are shown in Supplementary Fig. S3d & e. Ag NPs embedded in GG are clearly seen and the particle density is found to be $\sim 10^{11}$ #/cm^2.

FTIR spectra were recorded for the structural characterization of GG and GG/Ag nanocomposite in order to identify the significant functional groups of GG (Supplementary Fig. S9, Table S1). Shift in the absorbance peaks from 1426 to 1398 cm^{-1} suggests the binding of Ag ions with carbonyl groups of GG[55]. However, the shift in the alcoholic groups (1046 to 1024 cm^{-1}) suggest the reduction of the silver ions by the oxidation of the hydroxyl and carbonyl groups. Over all, it can be concluded that both hydroxyl and carbonyl groups of GG are involved in the synthesis of Ag nanoparticles[56].

Electrical conductivity of GG and GG/Ag nanocomposite film I was performed under ambient environment. Normal film (Film I) is obtained with 15 mM and the other film (film II) is prepared with 30 mM. Particle density of GG/Ag film (film II) is higher as compared to film I which indicates that the density can easily be varied by controlling the $AgNO_3$ concentration without disturbing the particle size. Conductivity of thin film of GG, (film I & II) was found to be 8.45×10^{-9}, 1.7×10^{-5} and 1.84×10^{-5} Ω^{-1}cm^{-1}, respectively. This clearly indicates that the conductivity of the films can be enhanced by increasing the loading of Ag nanoparticles in GG (Supplementary Fig. S10). Furthermore, the change in the conductivity of GG/Ag nanocomposites upon exposure to aqueous ammonia prompted us to explore the film as chemiresistor sensors and investigate the underlying mechanism. SEM image of film II after several measurements is shown in Supplementary Fig. S3f, which suggests that the films are stable to ammonia exposure. X-ray photoelectron spectroscopy (XPS) analysis has been carried out by using Kratos AXIS ULTRA DLD spectrometer.

Sensor measurements. Thin films of GG/Ag nanocomposite were formed on a flexible transparency slide (1 cm × 1 cm) by a drop-cast method and dried in air. Once the films are formed, Ag paste is used to make electrodes for electrical measurements. The optical micrograph of the film on a flexible substrate is shown in Fig. 2a. The sensor GG/Ag nanocomposite film with electrical leads is shown in the inset of Fig. 2a. An Agilent device Analyzer B1500A was employed to serve as both voltage source and current meter. Aqueous ammonia sensing experiments were carried out in a simple home-made testing chamber whose net volume ~800 cm^3 (10 cm × 10 cm × 8 cm) as shown in Fig. 2b. The distance of ammonia solution from sensor film is kept 1 cm. The concentrated ammonia vapors of different concentration were introduced into the testing chamber manually at the humidity of ~48% and temperature of 20–25°C.

In order to understand the sensing mechanism, we have carried out experiments under different environmental conditions (ambient, oxygen and nitrogen) and studied the field effect transistor (FET) characteristics of the sensing film on a Si/SiO_2 (300 nm thickness) substrate.

1. King, B. H., Gramada, A., Link, J. R. & Sailor, M. J. Internally referenced ammonia sensor based on an electrochemically prepared porous SiO_2 photonic crystal. *Adv. Mater.* **19**, 4044–4048 (2007).
2. Narasimhan, L. R., Goodman, W. & Patel, N. Correlation of breath ammonia with blood urea nitrogen and creatinine during hemodialysis. *Proc. Natl. Acad. Sci.* **98**, 4617–4621 (2001).
3. Sahm, M., Oprea, A., Barsan, N. & Weimar, U. Water and ammonia influence on the conduction mechanisms in polyacrylic acid films. *Sens. Actuators B* **127**, 204–209 (2007).
4. Pushkarsky, M. B., Webber, M. E., Baghdassarian, O., Narasimhan, L. R. & Patel, C. K. N. Laser-based photoacoustic ammonia sensors for industrial applications. *Appl. Phys. B* **75**, 391–396 (2002).
5. Timmer, B., Olthuis, W. & van den Berg, A. Ammonia sensors and their applications–a review. *Sens. Actuators B* **107**, 666–677 (2005).
6. Shen, C. Y. & Liou, S. Y. Surface acoustic wave gas monitor for ppm ammonia detection. *Sens. Actuators B* **131**, 673–679 (2008).
7. Christie, S., Scorsone, E., Persaud, K. & Kvasnik, F. Remote detection of gaseous ammonia using the near infrared transmission properties of polyaniline. *Sens. Actuators B* **90**, 163–169 (2003).
8. Ansari, S. G. *et al.* Urea sensor based on tin oxide thin films prepared by modified plasma enhanced CVD. *Sens. Actuators B* **132**, 265–271 (2008).
9. Ansari, S. G. *et al.* Glucose sensor based on nano-baskets of tin oxide templated in porous alumina by plasma enhanced CVD. *Biosens. Bioelectron.* **23**, 1838–1842 (2008).
10. Valentini, F., Biagiotti, V., Lete, C., Palleschi, G. & Wang, J. The electrochemical detection of ammonia in drinking water based on multi-walled carbon nanotube/

copper nanoparticle composite paste electrodes. *Sens. Actuators B* **128**, 326–333 (2007).
11. Wang, X., Miura, N. & Yamazoe, N. Study of WO_3-based sensing materials for NH_3 and NO detection. *Sens. Actuators B* **66**, 74–76 (2000).
12. Rout, C. S., Hegde, M., Govindraj, A. & Rao, C. N. R. Ammonia sensors based on metal oxide nanostructures. *Nanotechnology* **18**, 205504 (2007).
13. Abaker, M. *et al.* A highly sensitive ammonia chemical sensor based on α-Fe_2O_3 nanoellipsoids. *J. Phys. D: Appl. Phys.* **44**, 425401 (2011).
14. Rahman, M. M., Jamal, A., Khan, S. B. & Faisal, M. Characterization and applications of as-grown β-Fe_2O_3 nanoparticles prepared by hydrothermal method. *J. Nanoparticle Res.* **13**, 3789–3799 (2011).
15. Dubas, S. T. & Pimpan, V. Green synthesis of silver nanoparticles for ammonia sensing. *Talanta* **76**, 29–33 (2008).
16. Ding, M., Tang, Y., Gou, P., Reber, M. J. & Star, A. Chemical sensing with polyaniline coated single-walled carbon nanotubes. *Adv. Mater.* **23**, 536–540 (2011).
17. Kauffman, D. R. & Star, A. Carbon nanotube gas and vapor sensors. *Angew. Chem. Int. Ed.* **47**, 6550–6570 (2008).
18. Murray, B. J., Walter, E. C. & Penner, R. M. Amine vapor sensing with silver mesowires. *Nano Lett.* **4**, 665–670 (2004).
19. Du, N. *et al.* Porous indium oxide nanotubes: layer-by-layer assembly on carbon-nanotube templates and application for room-temperature NH_3 gas sensors. *Adv. Mater.* **19**, 1641–1645 (2007).
20. Zhang, D. *et al.* Doping dependent NH_3 sensing of indium oxide nanowires. *Appl. Phys. Lett.* **83**, 1845–1847 (2003).
21. Chang, R. L. J. & Yang, J. *para*-Mercaptobenzoic acid-modified silver nanoparticles as sensing media for the detection of ammonia in air based on infrared surface enhancement effect. *Analyst* **136**, 2988–2995 (2011).
22. Sandhu, A. Gas sensing: platinum platform. *Nature Nanotechnol.* doi:10.1038/nnano.2008.28.
23. Sberveglieri, G. Recent developments in semiconducting thin-film gas sensors. *Sens. Actuators B* **23**, 103–109 (1995).
24. Nicolas-Debarnot, D. & Poncin-Epaillard, F. Polyaniline as a new sensitive layer for gas sensors. *Anal. Chim. Acta* **475**, 1–15 (2003).
25. Lahdesmaki, I., Lewenstamand, A. & Ivaska, A. A polypyrrole-based amperometric ammonia sensor. *Talanta* **43**, 125–134 (1996).
26. Mun, S., Chen, Yi & Kim, J. Cellulose–titanium dioxide–multiwalled carbon nanotube hybrid nanocomposite and its ammonia gas sensing properties at room temperature. *Sens. Actuators B* **171–172**, 1186–1191 (2012).
27. Yavari, F. *et al.* High sensitivity gas detection using a macroscopic three-dimensional graphene foam network. *Sci. Rep.* **1**, 166 (2011).
28. Chen, G. *et al.* Enhanced gas sensing in pristine carbon nanotubes under continuous ultraviolet light illumination. *Sci. Rep.* **2**, 343 (2012).
29. Fowler, J. D. *et al.* Practical chemical sensors from chemically derived graphene. *ACS Nano* **3** (2), 301–306 (2009).
30. Dua, V. *et al.* All-organic vapor sensor using inkjet-printed reduced graphene oxide. *Angew. Chem. Int. Ed.* **49**, 2154–2157 (2010).
31. Johnson, J. L., Behnam, A., An, Y., Pearton, S. J. & Ural, A. Experimental study of graphitic nanoribbon films for ammonia sensing. *J. Appl. Phys.* **109**, 12 (2011).
32. Dan, Y. *et al.* Intrinsic response of graphene vapor sensors. *Nano Letters* **9**(4), 1472–1475 (2009).
33. Moon, H. G. *et al.* Self-activated ultrahigh chemosensitivity of oxide thin film nanostructures for transparent sensors. *Sci. Rep.* **2**, 588 (2012).
34. Pandey, S., Goswami, G. K. & Nanda, K. K. Green synthesis of biopolymer-silver nanoparticle nanocomposite: an optical sensor for ammonia detection. *Int. J. Bio. Macromolecules* **51**, 583–589 (2012).
35. Chiesa, M. *et al.* Reversible insulator-to-metal transition in p^+-type mesoporous silicon induced by the adsorption of ammonia. *Angew. Chem. Int. Ed.* **42**, 5032–5035 (2003).
36. Joseph, Y., Guse, B., Yasuda, A. & Vossmeyer, T. Chemiresistor coatings from Pt- and Au-nanoparticle/nonanedithiol films: sensitivity to gases and solvent vapors. *Sens. Actuators B.* **98**, 188–195 (2004).
37. Mitsudome, T. *et al.* Oxidant-free alcohol dehydrogenation using a reusable hydrotalcite-supported silver nanoparticle catalyst. *Angew. Chem. Int. Ed.* **47**, 138–141 (2008).
38. Besson, M. & Gallezot, P. Selective oxidation of alcohols and aldehydes on metal catalysts. *Catalysis Today* **57**, 127–141 (2000).
39. Kluytmans, J. H. J., Markusse, A. P., Kuster, B. F. M., Marin, G. B. & Schouten, J. C. Engineering aspects of the aqueous noble metal catalysed alcohol oxidation. *Catalysis Today* **57**, 143–155 (2000).
40. Brittian, H. G. Analytical profile of drug substances and excipients. **24**, pp. 246, Chapter. 6, Academic Press Inc. (1996).
41. Yamazoe, N., Fuchigami, J., Kishikawa, M. & Seiyama, T. Interactions of tin oxide surface with O_2, H_2O and H_2. *Surf. Sci.* **86**, 335 (1979).
42. Chen, Z. & Lu, C. Humidity Sensors: A Review of Materials and Mechanisms. *Sensor letters* **3**, 274–295 (2005).
43. Boyle, J. F. & Jones, K. A. The effects of CO, water vapor and surface temperature on the conductivity of a SnO_2 gas sensor. *J. electronic materials* **6**, 717–733 (1977).
44. Singh, A. K. *et al.* Bending stress induced improved chemiresistive gas sensing characteristics of flexible cobalt-phthalocyanine thin films. *Appl. Phys. Lett.* **102**, 132107 (2013).
45. Yao, K. *et al.* Towards one key to one lock: catalyst modified indium oxide nanoparticle thin film sensor array for selective gas detection. *J. Mater. Chem*, **22**, 7308 (2012).
46. Blazevic, N., Kolbah, D., Belin, B., Sunjić, V. & Kajfez, F. Hexamethylenetetramine. a versatile reagent in organic synthesis. *Synthesis* 161–176 (1979).
47. Chen, P.-L. & Chen, I.-W. Reactive cerium (IV) oxide powders by the homogeneous precipitation method. *J. Am. Ceram. Soc.* **76**, 1577–1583 (1993).
48. Liang, H., Raitano, J. M., Zhang, L. & Chan, S.-W. Controlled synthesis of Co_3O_4 nanopolyhedrons and nanosheets at low temperature. *Chem. Commun.* **2009**, 7569–7571 (2009).
49. Zhang, F. *et al.* Cerium oxide nanoparticles: Size-selective formation and structure analysis. *Appl. Phys. Lett.* **80**, 127–129 (2002).
50. Lu, C., Raitano, J. M., Khalid, S., Zhang, L. & Chan, S. Cubic phase stabilization in nanoparticles of hafnia-zirconia oxides: Particle-size and annealing environment effects. *J. Appl. Phys.* **103**, 124303 (2008).
51. Shetty, A. & Nanda, K. K. ZnO/poly(3,4-ethylenedioxythiophene) poly(styrenesulfo-nate) based ultraviolet and visible photodetectors: role of defects. *Mater. Exp.* **2**, 251–256 (2012).
52. Shetty, A. & Nanda, K. K. Tunable device properties of free-standing inorganic/organic flexible hybrid structures obtained by exfoliation. *Appl. Phys. Lett.* **100**, 242108 (2012).
53. Ahsanulhaq, Q., Kim, S. H. & Hahn, Y. B. A templateless surfactant-free seedless aqueous route to single-crystalline ZnO nanowires synthesis. *J. Phys. Chem. Solids* **70**, 627–631 (2009).
54. Wu, P.-Y., Pike, J., Zhang, F. & Chan, S.-W. Low-temperature synthesis of Zinc Oxide nanoparticles. *Int. J. Appl. Ceram. Technol.* **3**, 272–278 (2006).
55. Mohan, Y. M., Raju, K. M., Sambasivudu, K., Singh, S. & Sreedhar, B. Preparation of acacia-stabilized silver nanoparticles: a green approach. *J. Appl. Polym. Sci.* **106**(5), 3375–3381 (2007).
56. Kora, A. J., Sashidhar, R. B. & Arunachalam, J. Gum kondagogu (*Cochlospermum gossypium*): a template for the green synthesis and stabilization of silver nanoparticles with antibacterial application. *Carbohydrate Polymers* **82**(3), 670–679 (2010).

Acknowledgements

The author (SP) is thankful to Dr. D. S. Kothari Post doctoral fellowship scheme (DSKPDF) of University grant commission (UGC) for its generous financial support. The authors also acknowledge financial assistance of Department of Science and Technology (DST) for other financial support.

Author contributions

S.P. performed synthesis of GG/Ag nanocomposite film and characterizations. S.P. and G.K.G. perform sensor measurements. K.K.N. supervised the experiments and contributed to manuscript preparation. S.P., G.K.G. and K.K.N. analysed the data and wrote the manuscript. All authors discussed the progress of research and reviewed the manuscript.

Additional information

Supplementary information accompanies this paper at http://www.nature.com/scientificreports

Competing financial interests: The authors declare no competing financial interests.

How to cite this article: Pandey, S., Goswami, G.K. & Nanda, K.K. Nanocomposite based flexible ultrasensitive resistive gas sensor for chemical reactions studies. *Sci. Rep.* **3**, 2082; DOI:10.1038/srep02082 (2013).